Procedia Manufacturing

Volume 1, 2015, Pages 429–441

43rd Proceedings of the North American Manufacturing Research Institution of SME http://www.sme.org/namrc

Experimental and Numerical Analysis of Microstructure Evolution during Linear Friction Welding of Ti6Al4V

Gianluca Buffa[1a*], Davide Campanella[1b], Marco Cammalleri[1c], Antonino Ducato[1d], Antonello Astarita[2e], Antonino Squillace[2f], Sergio Esposito[3g] and Livan Fratini[1h]

[1]*Dept. of Chemical, Management, Computer Science and Mechanical Engineering University of Palermo, Italy*

[2]*Dept. of Chemical, Materials and Industrial Production Engineering, University of Naples, Italy*

[3]*Manufacturing and Assembly Research and Development, Alenia Aermacchi S.p.A., Italy*

[a]gianluca.buffa@unipa.it, [b]davide.campanella@unipa.it, [c]marco.cammalleri@unipa.it, [d]antonino.ducato@unipa.it, [e]antonello.astarita@unina.it, [f]squillac@unina.it, [g]sergio.esposito@alenia.it

Abstract

Linear Friction Welding (LFW) is a solid state welding process used to joint bulk components. In the paper, an experimental and numerical study on LFW of Ti6Al4V titanium alloy is presented. A laboratory designed LFW machine has been used to weld the specimens with different contact pressure and oscillation frequency. The joint microstructure has been experimentally observed with SEM and EDS. A dedicated numerical model, able to predict temperature, strain and strain rate distribution as well as the phase volume fraction evolution, has been utilized to predict the final microstructure in the welded parts. It was found that complete transformation of the alpha phase into beta phase occurs during the process. After cool down, martensitic structure is obtained at the core of the weld due to high temperatures reached during the process and high cooling rates occurring at the end of the reciprocating motion. Microhardness measurements confirmed increased hardness in the Weld Zone with respect to the parent material

Keywords: LFW, Ti-6Al-4V, Phase transformation, FEM.

* Corresponding author

Peer-review under responsibility of the NAMRI Scientific Committee

doi:10.1016/j.promfg.2015.09.053

1 Introduction

Linear Friction Welding (LFW) is a solid state welding process able to join two components, made out of same or different materials, by means of the heat created by friction generated at the contact interface (Li et al., 2014b). During the process different stages can be identified (Li et al., 2010b): first, during the initial stage, a reciprocating motion is given to one workpiece while a forging pressure is applied on the other. The combined action of pressure and friction forces work generates heat causing material softening, which is required to reach the proper plastic conditions at the contact interface and activate solid bonding. During the transition stage the actual contact surface between the two workpieces become 100% of the geometric surface due to the erosion of asperities. As the process goes on, part of the workpieces material is expelled from both the sides and the front of the specimens and an equilibrium stage is reached. Finally, the relative movement of the two parts is stopped and the normal pressure is increased (Vairis and Frost, 1998). After the last phase, the joint is cooled down in order to consolidate the welded zone. The heat generated during the process is controlled by regulating amplitude and frequency of the reciprocating motion (Vairis and Frost, 1999). The process has been demonstrated effective in welding similar and dissimilar joints of aluminum alloys, steels, nickel alloys and titanium alloys (Bhamji et al., 2011). In particular, the use of titanium alloys in aeronautic is remarkably increased in the last decades, both for engine and aero-structure components, thanks to their excellent mechanical properties, corrosion resistance and compatibility with CFRP (Li et al., 2014b). Traditional fusion welding hardly result in satisfying mechanical properties of the joint. LFW, as a solid-state welding process, can represent an effective solution.

The alloy under investigation in this research activity, i.e. Ti6Al4V, as an alpha beta alloy, may show different volume fractions of alpha and beta phases, depending on heat treatment and interstitial (primarily oxygen) content (Liu and Welsch, 1988). Moreover, it can be characterized by a variety of microstructures with different arrangements of the alpha and beta phases, depending on the particular thermo mechanical treatment experienced by the material. When the plastic deformation occurs below the beta transus temperature (about 980°C for the considered alloy) the final microstructure will be bimodal with alpha lamellae of smaller dimension. On the other hand, when the material is deformed at temperature in excess of the beta transus, a fully lamellar structure is obtained (Astarita et al., 2013c, Bruschi et al., 2004).

Due to the complexity of the process design because of the need to take into account, at the same time, technological, geometrical and metallurgical variables, the use of a numerical model can be very useful in the engineering of LFW of titanium alloys. Literature on LFW numerical modeling counts few papers (Vairis, 2012) and most of them consider the process as modeled by means of a 2D approach in which one of the joining samples is considered rigid and the process is split in two parts, considering the thermal aspect and the mechanical one as separated. Kiselyeva et al. (Kiselyeva et al., 2012) investigated the microstructural evolution of two α+β titanium alloys, VT6 and VT8M-1, undergone to a LFW process and used a 2D numerical analysis by means of ANSYS™ Mechanical code, in which the lower sample is constrained vertically and a pressure is assigned to the upper face of the top workpiece. Both samples were set at room temperature and the system was considered adiabatic due to short process time. The friction coefficient was considered increasing linearly with temperature up to 893 K. Results showed a good agreement between numerical simulation and experimental welding in the shape of the heat-affected zone. Turner at al. (Turner et al., 2011) carried out a 2D FE analysis with plane-strain mode of the LFW process of Ti-6Al-4V titanium alloy using a single deformable workpiece, modeled as the experimental sample part, and two rigid tooling dies having a U-shape in order to constrain the workpieces. A forging load is applied along the top surface of the workpiece, while lower workpiece is forced to oscillate in time with the lower die by the locking mechanism of the tooling surrounding the lower portion of the workpiece. The material characterization is made of a set of flow stress curve defined within the temperature and strain rate range involved within the process. This model is able to predict the most important thermal and

mechanical output variables of the process. Moreover, the deformation of the zone of complete contact between joining parts was observed. Yamileva et al. (Yamileva, 2012) proposed a FE analysis of the thermo-elastic deformations of LFW samples due to friction forces, using SIMULIA ABAQUS™ and ANSYS™ Mechanical systems. A sinusoidal law was assigned to move the top workpiece and, at the same time, a distributed force was applied to the top surface, while the bottom sample was maintained fixed within the workspace. The friction coefficient was considered as a function of temperature. Li et al. (Li et al., 2010a) (Li et al., 2013) proposed a 2D analysis of LFW process, using ABAQUS™ software, in which the geometry of workpiece is built as the experimental sample and shoes a rigid surface. The specimen meshing was carried out by means of 4-node elements with coupled thermo-mechanical calculation. Mesh density increased with decreasing distance from the specimens interface. The workpiece was allowed to move in the Y direction only, while the rigid surface was allowed to move in the X direction using a sinusoidal function with a given amplitude and frequency. The friction coefficient at the interface workpiece/die was defined as function of a temperature.

Although the use a 2D model simplifies the design of the simulation campaign because of an easy set-up of boundary conditions and quick computational times, the accuracy in prediction of thermo-mechanical behavior of a complex process like LFW significantly decreases. In fact, the use a 2D analysis in plain-stress condition to simulate a complex 3D process like LFW represents a considerable limitation because the material flow evolution within a 2D simulation is less accurate than a 3D analysis. As observed in (Li et al., 2014a), “LFW in 2D may not well reveal its bonding nature for the improper model simplifications or assumptions”. Additionally, boundary effects along the direction orthogonal to the oscillation one are not considered in 2D models. A limiting assumption commonly found in literature papers is the use of a “semi-rigid approach” in which only one sample is a deformable object while the other is modeled as rigid, thus introducing a mechanical behavior different from the real one. Based on the above observation it arises the necessity of developing a fully-coupled 3D analysis of LFW with both deformable objects.

In this paper, an experimental and numerical analysis of LFW of titanium alloys is presented. Three different case studies have been studied, at the varying of the pressure on the specimens, in order to obtain three different welding conditions, namely a cold joint, a sound joint, and a joint characterized by an excess of flash. The obtained joints have been analyzed and characterized form the metallurgical point of view. Finally, the developed numerical model was used to explain the behavior of the material during the process.

2 Materials and Methods

2.1 Experimental procedure

A laboratory machine for small scale LFWed parts was designed and developed, starting from the experience gained during experimental activities previously carried out by some of the authors (Fratini, 2013). This machine exploits a desmodromic kinematic chain in order to obtain the oscillation of the bottom specimen. Two interchangeable cams with different number of lobes, in order to widen the available range of oscillation frequency, were placed on the two parallel shafts connected by coupling belt and pulleys. An hydraulic actuator, fixed on a steel rack and controlled by an electro-valve, allows a load up to 15,000 kN. A hydraulic electro-valve, controlled by a virtual instrument, determines the beginning and the end of the test trial. The virtual instrument sets the pressure on the actuator in an assigned process time. A number of devices and sensors controlled by a unique interface were introduced to in-process monitor torque, acceleration and temperature, thus increasing the machine capabilities. A sketch of the main components of the machine is shown in Figure 1. A pneumatic clutch was positioned on a secondary shaft and connected to one of the cams in order to stop the reciprocating motion at the pre-determined process time. On the same secondary shaft line, a flywheel

was added to balance the effects of inertia. The flywheel was placed before the clutch thus obtaining a quick stop reducing the oscillating specimen inertia. During the experimental tests, varying oscillation frequency and applied pressure were used, while oscillation amplitude and process time were kept constant at 3 mm and 4 s, respectively.

In particular, the latter parameter was chosen on the basis of the results of preliminary experimental tests carried out to identify the conditions leading to an as wide as possible process window. The initial distance between the contact surfaces of the specimens was fixed to 0.5 mm. Before the test, the process time is selected through the virtual control instrument and, once the test started, the software controls the pneumatic clutch and consequently the test duration interrupting instantly the alternative motion after the process time is reached.

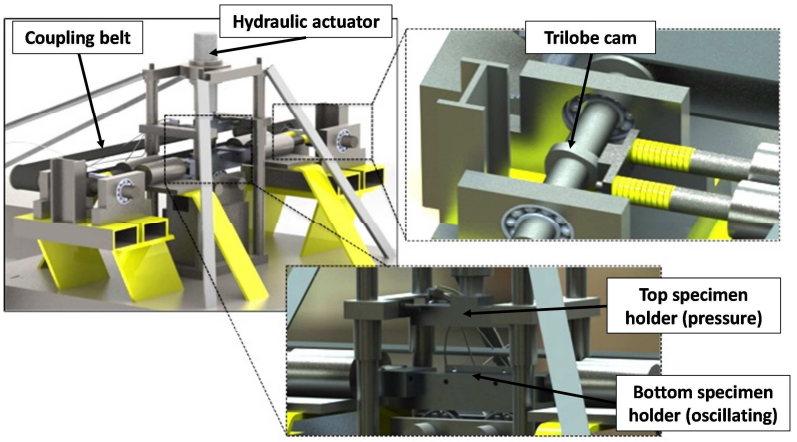

Figure 1: The LFW machine prototype

The specimens are characterized by height of 10 mm and cross-sectional dimensions at the contact interface equal to 10 mm x 7 mm. Each test was repeated three times showing excellent repeatability in terms of sound or poor weld obtained. Three case studies, characterized by a different combination of oscillation frequency and pressure, i.e. by different heat input, were considered. In this way, low, medium and high heat input into the welds were obtained (Table 1).

Case study	Frequency f [Hz]	Pressure p [MPa]
Low	36	20
Medium	**36**	**30**
High	45	40

Table 1: Considered case studies

The test characterized by the pressure and frequency values of 30 MPa and 36 Hz, respectively, resulted in a sound joint and was considered as reference conditions. Figure 2 shows the welded joints obtained for the three case studies.

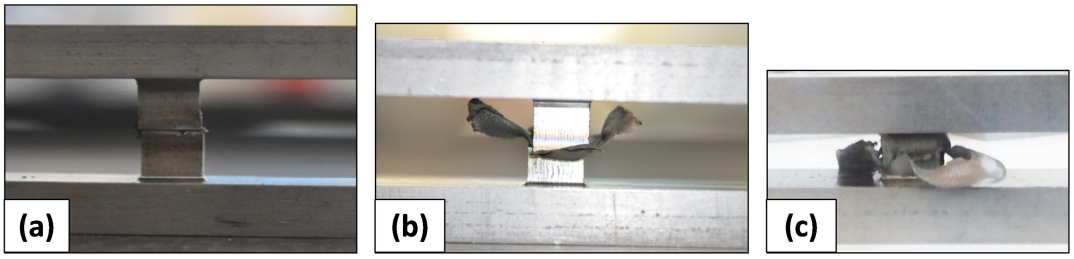

Figure 2: Welds obtained with (a) low, (b) medium and (c) high heat input

The used material is Ti6Al4V titanium alloy. Figure 3 shows the microstructure of the parent material characterized by a biphasic structure (α+β) with α equiaxed grains and intergranular β phase. The EDS analysis (see magnified part of Figure 3) highlights the chemical composition as well as the brighter areas, namely the β-phase, rich in β stabilizing elements (vanadium and iron), and the darker areas, rich in aluminum, namely the α-phase.

The specimens for the metallographic analysis were prepared according to ASTM E3-11 standard procedures and etched with 0.5% HF solution. Observations were carried out using scanning electron microscopy (SEM), the elemental analysis was performed using EDS. Vickers micro-hardness measurements were performed to evaluate the modifications induced by the welding process in the different zones of the joint.

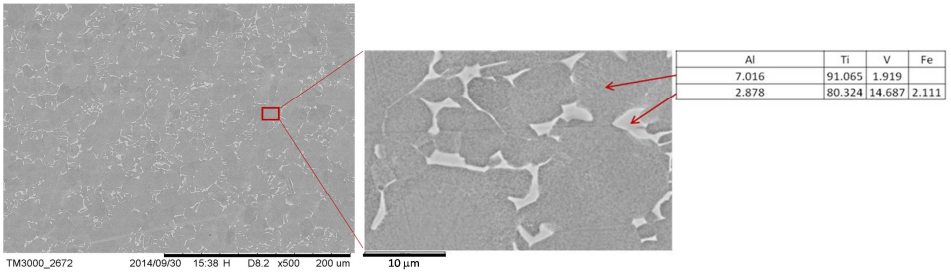

Figure 3: Microstructure of the as received Ti6al4V

2.2 Numerical model set-up

The simulation campaign was carried out using a thermo-mechanically coupled 3D model with both deformable samples having the same dimensions of the real specimens (Figure 4).

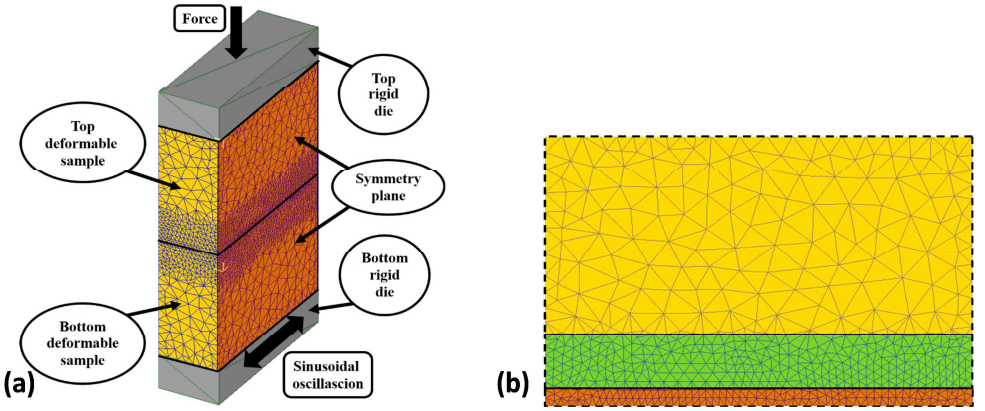

Figure 4: (a) 3D view of specimens with symmetry plane and movement directions; (b) front view of workpiece with mesh distribution with element size zones: yellow 1.2 mm, green 0.3 mm, orange 0.15 mm

Unlike the semi-rigid simulations, in which only one sample is modeled as deformable while the other is a rigid object, this approach considers the mutual actions between both parts during the process. Each sample was modeled taking into account the terminal part of the real samples, without considering those areas having the role of structural part for proper clamping (Figure 4 a). This assumption can be accepted considering the extremely low thermal conductivity of the considered titanium alloy. Due to the geometrical symmetry of the process, a symmetry plane was placed along the oscillating direction in order to simulate half of each object, reducing the computational cost in 3D. Each simulated sample has 10x3.5x7 mm dimensions and was discretized using tetrahedral element mesh with a different size on the main areas in order to better simulate the material flow mechanism causing the friction extrusion of material, thus optimizing the calculation time. In particular, two different mesh windows with increasing element density were used for the discretization of the contact region (Figure 4 b). The mesh of the farthest area form the contact interface includes elements having a size of about 1.2 mm, the middle green zone is meshed using elements with a fixed size of 0.3 mm, while the contact orange zone is meshed using elements with a fixed size of 0.15 mm. This mesh set-up resulted in about 32000 elements per sample.

A fixed time-step of 0.0001 sec was used in all simulations. The choice of this small value, although resulting in increased CPU time, was driven form the need to correctly follow the fast movement of the oscillating specimen.

All thermal boundary conditions were defined taking into account both the process nature and the used material properties. The process were considered as adiabatic as the process length, i.e. 4 sec, does not allow significant heat transfer phenomena with external air. Due to the LFW process mechanics, the thermal exchange coefficient at the contact interface typically used for forging processes was used. In particular, a heat exchange coefficient of 11 N/s/mm/°C was selected. No heating induction window was used to pre-heat the material and every analysis started at room temperature. The friction conditions were simulated using the shear model. Prior simulations showed some instability in using a temperature dependent friction coefficient due to the coupled calculation. In the experimental studies of Schroeder at al. (Schröder et al., 2014) on LFW process of Ti-6Al-4V, a mean value of the friction factor equal to 0.55 was measured during the experiments while a peak value of about 0.7 was observed. In this paper, the authors considered a fixed value of 0.55. No constrained nodes were considered to limit the material flow of the free surfaces of the specimen as well as no rigid bodies with U-shape to guide each sample was modeled, while sticking condition were used at each die/workpiece interface in order to guide each sample by means of assigned die movements.

The thermo-mechanical characterization of TI-6Al-4V alloy within the numerical code was defined as a flow stress curves set (Ducato et al., 2014, Astarita et al., 2013a, Ducato et al., 2013a, Astarita et al., 2013b) using the data coming from the JMatPro™ Demo database for a wide range of temperature and strain rates. The material definition was extended with a de-coupled phase change kinetics integration for volume fraction calculation during the process. Alpha-to-Beta phase evolution was based on an Avrami generalized model (Sha and Malinov, 2009) while the Beta-to-Alpha+Beta transformation was assigned by means of an Avrami equation using the TTT start curve of the considered alloy and a mean value of literature experimental data for Avrami number (Ducato et al., 2014, Astarita et al., 2013a, Ducato et al., 2013a, Astarita et al., 2013b). Finally, a thermal conductivity of Ti-6Al-4V alloy as function of temperature was used (Ducato et al., 2013b). As far as the movement and pressure boundary conditions are concerned, they have been assigned to the rigid dies, which, in turn, have a sticking contact constraint with the deformable bodies. This choice was made in order to avoid numerical instabilities arising when the same movement and pressure boundary conditions are assigned to the deformable objects.

3 Results

First, the results of the numerical model are presented. Figure 5 shows the final shape of the specimens at the end of the simulation, i.e. after 4 s, for the reference conditions. It should be noticed that in LFW of titanium alloys, a very thin flash is extruded form the lateral surface of the specimens (see again Figure 2 b and c). In order to properly model the flash, an extremely fine mesh has to be used, resulting in a significant increase of the elements used for each specimen and, consequently, in unaffordable CPU times. For this reason, the flash has been manually removed every 0.3 s from the deformable objects.

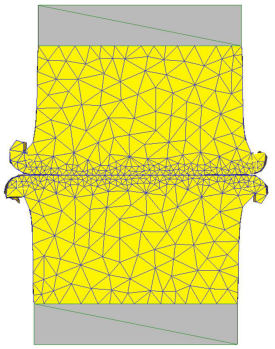

Figure 5: Final shape of the specimens at the end of simulation after flash removal (medium case study)

Figure 6 shows the temperature distribution in the medium case study specimen for bottom view and lateral view (symmetry plane side). It is seen that peak temperature, equal to about 925°C, is reached at the center of the specimen. It is important noticing that this temperature value is close to the beta transus temperature of Ti6Al4V. at the contact surface periphery, lower temperature is calculated, with a drop of about 200°C. This result, consistent with what found in (Sorina-Muller et al., 2010), is due to the very short time of overlap and to the losses via convection. Based on the obtained temperature values, at least partial transformation of the alpha phase in beta phase is expected during the process. Additionally, due to the low thermal conductivity of the used titanium alloy, temperature

quickly decreases along the specimen height, being equal to about the half of the peak temperature at a distance of 5 mm from the contact interface.

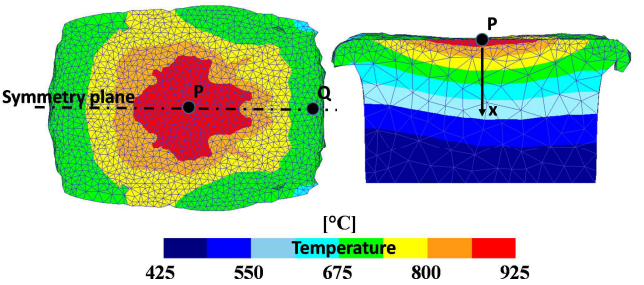

Figure 6: Temperature distribution for the medium case study: contact surface and lateral view (symmetry plane side)

The temperature histories calculated for the three case studies for a point located at the center of the contact interface (see point P in Figure 6) are reported in Figure 7. Similar temperature evolution is calculated for the three case studies at the center of the contact interface. A rapid increase of the temperature is obtained. A slight drop of temperature occurs in the specimen when the flash extrusion begins due to the heat lost with the flash itself. Then, during the equilibrium stage, temperature slightly increases again until the maximum value is reached. As far as the medium case study is concerned, maximum temperature during the process exceeds the beta transus temperature. In turn, for the low cases study, maximum temperature is always below 900°C. As expected, the high case study shows the largest values of temperature, reaching about 1200°C during the process.

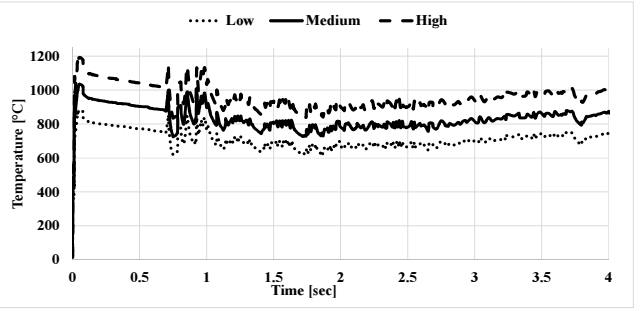

Figure 7: Temperature histories for point P for the three considered case studies

As described in the paragraph 2.2, the utilized numerical model is able to predict the phase distribution during the process. Figure 8 shows the alpha and beta phase distribution at the end of the welding process.

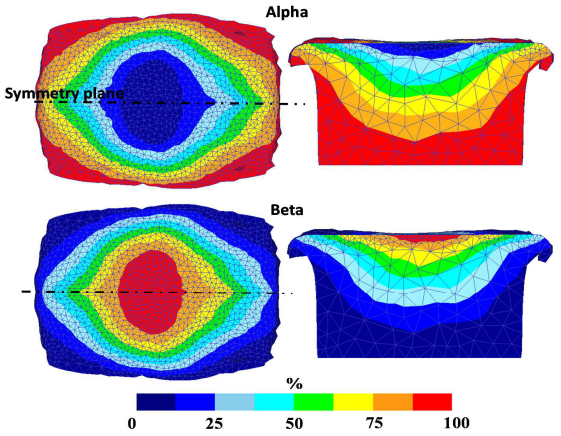

Figure 8: Alpha and beta phase distribution for the medium case study: contact surface and lateral view (symmetry plane side)

It is noted that complete transformation into the beta phase is reached, for the medium case study, at the core of the contact interface. Phase volume fraction values larger than 50% are obtained in most of the contact area (please note that the bottom view include also the longitudinal and transversal flash). However, the thickness of the beta phase layer is quite small due to the steep temperature decrease with increasing distance from the contact surface. In this way, in most of the specimen large areas of untransformed alpha phase is observed. In particular, at about mid height of the specimen 75% of alpha phase is calculated.

After the reciprocating motion stops, the specimens cool down to room temperature due to the thermal exchange with environment. This step was simulated with the developed model in order to predict the final microstructure in the welded joints. Figure 9 shows the temperature vs time curve during cool down for the medium case study (point P). A rapid drop of temperature takes place during the very first seconds after the process ending. In particular, cooling rates higher than 250°C/s are calculated at the beginning of the cool down process. This is also due to the small dimension of the utilized specimens. After about 4 s, the cooling rate significantly decreases and assumes a constant value.

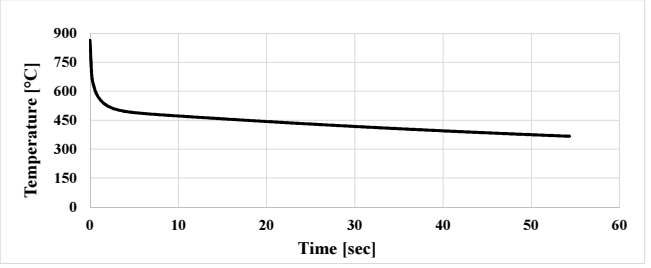

Figure 9: Temperature vs time during cool down (medium case study, point P)

The evolution of the phase volume fraction during the process and the subsequent cool down is shown in Figure 10.

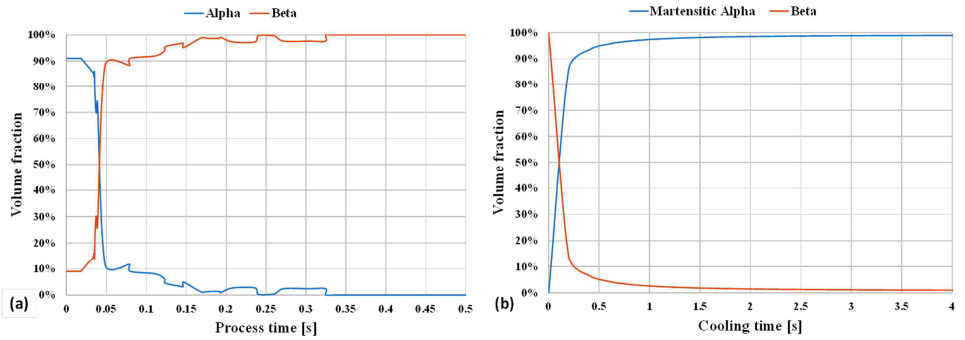

Figure 10: Phase volume fraction evolution during (a) welding and (b) cool down (medium case study, point P)

Due to the high temperatures reached at the beginning of the process, the alpha phase rapidly transforms into beta phase. When the reciprocating motion stops, the extremely high cooling rate prevent the transformation of beta phase into alpha+beta structure. Indeed, martensitic alpha is formed with a phase volume fraction equal to about 100%, for the considered observation point, within the first few seconds.

The microstructural analysis of the welded joints along the x axis (see again Figue 6) revealed three distinct zones: the parent material (PM), the weld zone (WZ), and a thermo-mechanically affected zone (TMAZ). Figure 11 shows the transition between the three areas for the medium case study. The, the narrow region between the phase-transformed weld bead and the parent material is the above-mentioned TMAZ. This zone is characterized by the presence of elongated beta lamellae with intergranular alpha, as illustrated in Figure 11b. The results of EDS analysis carried out in the TMAZ reveal both an α-phase (the darker part in the figure) and a β-phase (the brighter part in the figure) stabilized by the presence of large amount of Aluminum and Vanadium, respectively. As the distance from the contact interface between the specimens decreases a further change in the microstructure is found. At higher magnification, the weld zone shows a microstructure characterized by martensitic phase (Karadge et al., 2007) (Figure 11c), thus confirming the numerical prediction. The high temperatures experienced during the joining process and the high cooling rate after linear friction welding caused the martensitic transformation. The chemical composition of the martensitic structure is, as expected, coincident with the nominal composition of the parent titanium alloy: due to the efficient stirring of the material, and the subsequent homogenization, the α-phase is not easily distinguishable by β-phase. A different microstructure is observed at the periphery of the contact surface. In figure 12, the micrograph of point Q (see Figure 6) is shown. A bimodal microstructure, characterized by globular alpha grains and alpha/beta lamellae is found. The non-complete transformation of the globular alpha into beta during the process indicates that the beta transus temperature was not reached. In this way, only the fraction of beta present in this area at the end of the process can transform into alpha/beta lamellae during the cool down.

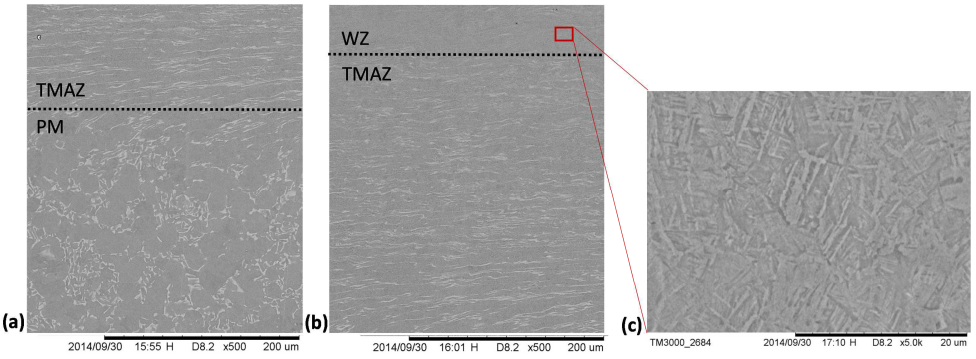

Figure 11: Micrographs of the medium case study along the x axis: (a) transition between parent material and TMAZ; (b) transition between TMAZ and weld zone; (c) magnification of the weld zone microstructure

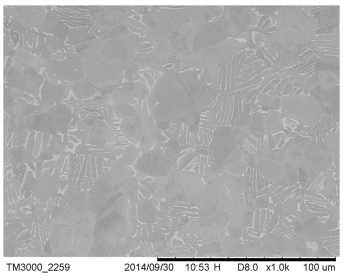

Figure 12: Micrographs of point Q (see Figure 6) of the medium case study

Finally, Vickers micro-hardness measurements were carried out in the three different zones of the specimen (Table 2). The indentations were performed with an applied load of 200 g; at least six valid measurements were performed within each single zone. The choice of the applied loads was made according to the microstructure of the different zones of the joint, in order to have all the indentations large enough to avoid that some inhomogeneities typical of the α + β alloys could affect the measurements. The results of micro-hardness confirm the SEM analysis: the martensitic transformation occurred in the weld bead results in increased of hardness. The micro-hardness values slightly return to those typical of the parent alloy as the distance from the weld bead increases. These values are consistent with the HV measurements carried out on Friction Stir Welded specimens of the same material (Buffa et al., 2013), in which the material undergoes analogous thermo-mechanical solicitation.

Indentation Nr	WZ	TMAZ	PM
1	382.80	367.42	316.47
2	372.09	358.62	362.45
3	390.66	360.41	333.91
4	399.54	360.56	361.23
5	390.57	352.16	329.40
6	372.74	357.09	364.93
Mean values	384.73	359.38	344.73

Table 2: HV measurements for the medium heat input case study

4 Conclusions

In the paper, the results of an experimental and numerical study on Linear Friction Welding of Ti6Al4V titanium alloy are presented. Three different case studies have been considered with varying contact pressure and oscillation frequency, leading to a cold weld, a sound joint and an excessive flash, respectively. A dedicated numerical model, able to predict the distribution of the main field variables as well as the phase volume fraction evolution during the process and the subsequent cool down, was utilized. Form the obtained results it can be stated that, when proper process parameters are used, a sound weld can be produced. The weld is characterized by martensitic microstructure in the weld zone. This is due to the high temperatures, in excess of the beta transus, reached during the process and to the extremely rapid cool down taking place after the reciprocating motion stops. Consequently, microhardness values higher than the ones of the base material are found in the weld zone. Finally, the thickness of the weld zone and of the TMAZ is limited due the extremely poor thermal conductivity of the utilized titanium alloy. In this way, no microstructural modification is found at a distance of about 5 mm form the contact interface between the specimens.

5 References

Astarita, A., Ducato, A., Fratini, L., Paradiso, V., Scherillo, F., Squillace, A., Testani, C. & Velotti, C. 2013a. Beta forging of Ti-6Al-4V: Microstructure evolution and mechanical properties. *Key Engineering Materials.*

Astarita, A., Ducato, A., Fratini, L., Paradiso, V., Scherillo, F., Squillace, A., Testani, C. & Velotti, C. 2013b. Beta Forging of Ti-6Al-4V: microstructure evolution and mechanical properties. *Current State-of-the-Art on Material Forming: Numerical and Experimental Approaches at Different Length-Scales, Pts 1-3,* 554-557**,** 359-371.

Astarita, A., Durante, M., Langella, A. & Squillace, A. 2013c. Elevation of tribological properties of alloy Ti-6% Al-4% v upon formation of a rutile layer on the surface. *Metal Science and Heat Treatment,* 54**,** 662-666.

Bhamji, I., Preuss, M., Threadgill, P. L. & Addison, A. C. 2011. Solid state joining of metals by linear friction welding: A literature review. *Materials Science and Technology,* 27**,** 2-12.

Bruschi, S., Poggio, S., Quadrini, F. & Tata, M. E. 2004. Workability of Ti-6Al-4V alloy at high temperatures and strain rates. *Materials Letters,* 58**,** 3622-3629.

Buffa, G., Ducato, A. & Fratini, L. 2013. FEM based prediction of phase transformations during Friction Stir Welding of Ti6Al4V titanium alloy. *Materials Science and Engineering A,* 581**,** 56-65.

Ducato, A., Fratini, L. & Micari, F. 2013a. Coupled thermo-mechanical-metallurgical analysis of an hot forging process of titanium alloy. *Current State-of-the-Art on Material Forming: Numerical and Experimental Approaches at Different Length-Scales, Pts 1-3,* 554-557**,** 638-646.

Ducato, A., Fratini, L. & Micari, F. 2013b. Coupled thermo-mechanical-metallurgical analysis of an hot forging process of titanium alloy. *Key Engineering Materials.*

Ducato, A., Fratini, L. & Micari, F. 2014. Prediction of phase transformation of Ti-6Al-4V titanium alloy during hot-forging processes using a numerical model. *Proceedings of the Institution of Mechanical Engineers Part L-Journal of Materials-Design and Applications,* 228**,** 154-159.

Fratini, L., Buffa, G., Cammalleri, M., Campanella, D. 2013. On the linear friction welding process of aluminum alloys: Experimental insights through process monitoring. *CIRP Annals - Manufacturing Technology,* 62**,** 295-298.

Karadge, M., Preuss, M., Lovell, C., Withers, P. J. & Bray, S. 2007. Texture development in Ti-6Al-4V linear friction welds. *Materials Science and Engineering A,* 459**,** 182-191.

Kiselyeva, S., Yamileva, A., Karavaeva, M., Nasibullayev, I. S., Bychkov, V., Medvedev, A. Y., Supov, A., Musin, F., Alexandrov, I. & Latysh, V. 2012. Computer modelling of linear friction welding based on the joint microstructure. *Journal of Engineering Science and Technology Review,* 5**,** 44-47.

Li, W.-Y., Ma, T. & Li, J. 2010a. Numerical simulation of linear friction welding of titanium alloy: Effects of processing parameters. *Materials & Design,* 31**,** 1497-1507.

Li, W., Shi, S., Wang, F., Ma, T., Li, J., Gao, D. & Vairis, A. 2013. Heat reflux in flash and its effect on joint temperature history during linear friction welding of steel. *International Journal of Thermal Sciences,* 67**,** 192-199.

Li, W., Wang, F., Shi, S., Ma, T., Li, J. & Vairis, A. 2014a. 3D Finite Element Analysis of the Effect of Process Parameters on Linear Friction Welding of Mild Steel. *Journal of Materials Engineering and Performance,* 23**,** 4010-4018.

Li, W. Y., Ma, T. J. & Li, J. L. 2010b. Numerical simulation of linear friction welding of titanium alloy: Effects of processing parameters. *Materials & Design,* 31**,** 1497-1507.

Li, W. Y., Vairis, A. & Ward, R. M. 2014b. Advances in Friction Welding. *Advances in Materials Science and Engineering*.

Liu, Z. & Welsch, G. 1988. Effects of oxygen and heat treatment on the mechanical properties of alpha and beta titanium alloys. *Metallurgical Transactions A,* 19**,** 527-542.

Schröder, F., Ward, R., Walpole, A., Turner, R., Attallah, M., Gebelin, J. & Reed, R. 2014. Linear friction welding of Ti6Al4V: experiments and modelling. *Materials Science and Technology*.

Sha, W. & Malinov, S. 2009. *Titanium Alloys: Modelling of Microstructure, Properties and Applications*.

Sorina-Muller, J., Rettenmayr, M., Schneefeld, D., Roder, O. & Fried, W. 2010. FEM simulation of the linear friction welding of titanium alloys. *Computational Materials Science,* 48**,** 749-758.

Turner, R., Gebelin, J. C., Ward, R. M. & Reed, R. C. 2011. Linear friction welding of Ti-6Al-4V: Modelling and validation. *Acta Materialia,* 59**,** 3792-3803.

Vairis, A. 2012. Mathematical Modelling of the Linear Friction Welding Process. *Journal of Engineering Science and Technology Review,* 5**,** 25-31.

Vairis, A. & Frost, M. 1998. High frequency linear friction welding of a titanium alloy. *Wear,* 217**,** 117-131.

Vairis, A. & Frost, M. 1999. On the extrusion stage of linear friction welding of Ti6Al4V. *Materials Science and Engineering a-Structural Materials Properties Microstructure and Processing,* 271**,** 477-484.

Yamileva, A. M., Yuldashev, A.V., Nasibullayev I.Sh., I.S. 2012. Comparison of the Parallelization Efficiency of a Thermo-Structural Problem Simulated in SIMULIA Abaqus and ANSYS Mechanical. *Journal of Engineering Science and Technology Review,* 5**,** 39-43.